# Design of high-temperature superconductors at moderate pressures by alloying AlH<sub>3</sub> or GaH<sub>3</sub>

Xiaowei Liang, <sup>1,2</sup> Xudong Wei, <sup>1</sup> Eva Zurek, <sup>3</sup>Aitor Bergara, <sup>4,5,6</sup> Peifang Li, <sup>7</sup> Guoying Gao, <sup>1, a)</sup> Yongjun Tian <sup>1</sup>

<sup>1</sup>Center for High Pressure Science (CHiPS), State Key Laboratory of Metastable Materials Science and Technology, Yanshan University, Qinhuangdao, Hebei, 066004, China

<sup>2</sup>School of Materials Science and Engineering, Henan University of Technology, Zhengzhou, 450001, China

<sup>3</sup>Department of Chemistry, State University of New York at Buffalo, Buffalo, New York 14260-3000, United States

<sup>4</sup>Physics Department and EHU Quantum Center, University of the Basque Country, UPV/EHU, 48080 Bilbao, Spain

<sup>5</sup>Donostia International Physics Center (DIPC), 20018 Donostia, Spain

<sup>6</sup>Centro de Física de Materiales CFM, Centro Mixto CSIC-UPV/EHU, 20018 Donostia, Spain

<sup>7</sup>Extreme Conditions Physics Research Team, College of Mathematics and Physics, Inner Mongolia Minzu University, Tongliao 028043, China

# a) Authors to whom correspondence should be addressed: gaoguoying@ysu.edu.cn

#### **ABSTRACT**

Since the discovery of hydride superconductors, a significant challenge has been to reduce the pressure required for their stabilization. In this context, we propose that alloying could be an effective strategy to get this. We focused on a series of alloyed hydrides with the AMH<sub>6</sub> composition, which could made via alloying A15 AH<sub>3</sub> (A=Al and Ga) with M (M=IIIB and IVB group metals), and studied their behavior under pressure. According to the research, seven of them were predicted to maintain the A15-type structure, similar to AH<sub>3</sub> under pressure, providing a platform for studying the effects of alloying on the stability and superconductivity of AH<sub>3</sub>. Among them, the A15-type phases of AlZrH<sub>6</sub> and AlHfH<sub>6</sub> were found to be thermodynamically stable in the pressure range of 40-150 and 30-181 GPa, respectively. Furthermore, they remain dynamically stable at even lower pressures, as low as 13 GPa for AlZrH<sub>6</sub> and 6 GPa for AlHfH<sub>6</sub>. These pressures are significantly lower what is required for stabilizing A15

AlH<sub>3</sub>. Additionally, the introduction of Zr and Hf into the alloys increases the electronic density of states at the Fermi level compared to AlH<sub>3</sub>. This enhancement leads to higher critical temperatures (*T<sub>c</sub>*) of 75 and 76 K for AlZrH<sub>6</sub> and AlHfH<sub>6</sub> at 20 and 10 GPa, respectively. In the case of GaMH<sub>6</sub> alloys, where M represents Sc, Ti, Zr or Hf, these metals reinforce the stability of the A15-type structure and reduce the lowest thermodynamically stable pressure for GaH<sub>3</sub>, from 160 GPa to 116, 95, 80 and 85 GPa, respectively. Particularly noteworthy is the A15-type GaMH<sub>6</sub> alloys, which remain dynamically stable at low pressures of 97, 28, 5 and 6 GPa, simultaneously exhibiting high *T<sub>c</sub>*s of 88, 39, 70 and 49 K at 100, 35, 10 and 10 GPa, respectively. Overall, these findings enrich the family of A15-type superconductors and provide insights for the future exploration of high-temperature hydride superconductors that can be stabilized at lower pressures.

#### I. INTRODUCTION

In recent years, hydrides have emerged as potential materials in the search of room-temperature superconductivity, not only from theoretical predictions<sup>1-5</sup> but also from experimental verifications.<sup>6-22</sup> In 2015, the predicted cubic H<sub>3</sub>S was synthesized for the first time and was experimentally confirmed to have a  $T_c$  of 203 K at 155 GPa.<sup>7,8</sup> Four years later, the  $T_c$  record passed to the LaH<sub>10</sub> metal hydride with an H-clathrate structure, which was observed to have  $T_c$  values of 250-260 K at 170-190 GPa.<sup>9,10</sup> Metallic clathrate hydrides were predicted to be a large class<sup>23-28</sup> and some of the predicted superconductors in this family have been successively verified experimentally, such as ThH<sub>9/10</sub> (146/161 K at 170-175 GPa),<sup>11</sup> YH<sub>6</sub> (224 K at 166 GPa; 220 K at 183 GPa),<sup>12,13</sup> YH<sub>9</sub> (243K at 201 GPa; 262 K at 182 GPa)<sup>13,14</sup> and CaH<sub>6</sub> (215 K at 172 GPa; 210 K at 160 GPa).<sup>15,16</sup> These achievements have greatly encouraged the exploration of room-temperature superconductivity in hydrides.

However, the possible application of superconducting hydrides is not only influenced by the superconducting transition temperature, as in the case of other superconductors, but also by the stabilization pressure. Although the hydrides mentioned above have high  $T_c$  values, the pressures required to stabilize them are also extremely high (> 150 GPa). Therefore, it is essential to obtain superconducting hydrides that are stable at low pressures. Our previous study proposed that the introduction of light B into the La-H system leads to a stable Fm3m LaBH<sub>8</sub> phase with BH<sub>8</sub> units, <sup>29-31</sup> which remains dynamically stable at 55 GPa and exhibits a  $T_c$  of 155 K. Subsequently, some other B, C and Si-based ternary hydrides were also estimated to show a good superconductivity at moderate pressures.<sup>32-35</sup> In these hydrides, the covalent units formed by including light elements with H contribute significantly to their low-pressure stability. Furthermore, the La-Y alloy tetrahydride was synthesized at 110 GPa, exhibiting a  $T_c$  of 92 K, and can be recovered at 80 GPa, both of which are lower pressure thresholds than those required for the synthesis of YH<sub>4</sub>. <sup>18</sup> Bi et al. synthesized the (La,Ce)H<sub>9</sub> alloy at megabar pressures of 97-172 GPa, which exhibited a  $T_c$  of 148–178 K.<sup>19</sup> More recently, the metastable compound  $P6_3/mmc$ -LaH<sub>10</sub> was stabilized at 146 GPa by introducing Al atoms to form  $P6_3/mmc$ -(La,Al)H<sub>10</sub>, with a  $T_c$  of 178 K.<sup>20</sup> An increase in the configurational entropy of a mixed alloy hydride will decrease its Gibbs free energy and enhance its stability. Therefore, alloying binary metal hydrides may be an alternative approach to optimize the stabilization pressure of superconducting hydrides.

Trihydrides are commonly found in binary metal hydrides and their superconductivity under pressure has been extensively studied. 36-45 Based on their structures, common metal trihydrides can be divided into two categories, one with the  $Pm\bar{3}n$  structure and the other with the  $Fm\bar{3}m$  structure. This provides a platform to tune the stability and superconductivity of hydrides by alloying. The  $Pm\bar{3}n$  structure, also called the A15 structure, is well known for its excellent superconducting performance. To date, about 50 alloys with this structure are superconductors, and some of them remain the most promising materials for practical applications. 46 Among binary hydrides, AlH<sub>3</sub>, GaH<sub>3</sub>, ZrH<sub>3</sub> and HfH<sub>3</sub> were predicted to become stable in the A15 structure at 73, 160, 8 and 27 GPa, respectively, in which metal atoms form a bodycentered cubic (bcc) lattice with the six H atoms occupying half of the tetrahedral interstices of the bcc lattice. 36-40 Interestingly, the A15 phase of AlH3 and ZrH3 were confirmed in experiments at 100 and 30 GPa, respectively, however, they do not present high values of  $T_c^{37,39,41}$  On the other hand, the Al5 phase of GaH<sub>3</sub> was estimated to have the highest T<sub>c</sub> of 102 K at 120 GPa.<sup>38</sup> However, A15 GaH<sub>3</sub> presents relatively high minimum pressures of ~160 and ~84 GPa for thermodynamic and dynamic stability respectively, <sup>38,47</sup> making its synthesis difficult. Below 160 GPa, A15 GaH<sub>3</sub> becomes thermodynamically unstable and transforms into a structure containing H<sub>2</sub> units, with an insulating character.<sup>26</sup> Comparing to Al and Ga, IIIB and IVB group metal atoms are less electronegative and could transfer more electrons to H<sub>2</sub> units, allowing structures with atomic hydrogens to remain stable at lower pressures. In addition, IIIB and IVB group metals can also exist in the trivalent state and form trihydrides. Therefore, alloying AlH<sub>3</sub>/GaH<sub>3</sub> with IIIB /IVB group metals could give stable alloy hydrides with the A15-type structure and the expected superconductivity at low pressures. For ternary

hydrides, A15-type GaAsH<sub>6</sub> and YZrH<sub>6</sub> were predicted to have *T<sub>c</sub>* values of 98 and 16 K at 180 GPa and ambient pressure, respectively.<sup>28, 48</sup> Recently, our group designed a series of A15 ternary hydrides, with the CaSnH<sub>6</sub> alloy demonstrating the lowest thermodynamically stable pressure of 110 GPa,<sup>47</sup> which also facilitated our exploration of ternary alloy hydrides. To some extent, alloying AlH<sub>3</sub>/GaH<sub>3</sub> with IIIB /IVB group metals also provides a way to control the physical properties of ternary hydrides through the choice of their constituent elements.

In this work, we investigate theoretically the structure, stability and superconductivity of alloy hydrides with the AMH<sub>6</sub> composition (A=Al and Ga; M= IIIB and IVB group metals). We chose the AMH<sub>6</sub> composition because the substitution of an M atom for an A atom in the A<sub>2</sub>H<sub>6</sub> unit cell is one of the most intuitive ways to form alloy hydrides. Furthermore, considering the promoting effect of configurational entropy in material formation, mixing metal elements in equal proportions may yield a highly disordered alloy hydride, making it more favorable for experimental synthesis. The results show that seven ternary hydrides, AlMH<sub>6</sub> (M=Ti, Zr and Hf) and GaMH<sub>6</sub> (M=Sc, Ti, Zr and Hf) are identified to be stable in the A15 structure. A15 AlZrH<sub>6</sub>, AlHfH6 and all GaMH6 are thermodynamically stable at pressures much lower pressures than those required to stabilize A15 AlH<sub>3</sub> and GaH<sub>3</sub>. Except for GaScH<sub>6</sub>, all of these hydrides also have significant advantages over AlH<sub>3</sub> and GaH<sub>3</sub> in terms of the lowest dynamically stable pressures, with AlZrH<sub>6</sub>, AlHfH<sub>6</sub>, GaZrH<sub>6</sub> and GaHfH<sub>6</sub> able to maintain their dynamical stability at ~13, 6, 5 and 6 GPa, respectively. Electronphonon coupling (EPC) calculations show that all of these ternary hydrides are superconducting. Among them, the estimated T<sub>c</sub> values for AlZrH<sub>6</sub>, AlHfH<sub>6</sub>, GaScH<sub>6</sub>, GaZrH<sub>6</sub> and GaHfH<sub>6</sub> are 75, 76, 88, 70 and 49 K at 20, 10, 100, 10 and 10 GPa, respectively. In addition, AlScH<sub>6</sub> and AlYH<sub>6</sub> are predicted to be stable in structures similar to  $Fm\overline{3}m$  Sc(Y)H<sub>3</sub> and they are also potential superconductors under pressure. Our results indicate that they have great potential to explore low-pressure stable high- $T_c$  superconductors in alloy hydrides.

### II. COMPUTATIONAL DETAILS

Structure searches of AMH<sub>6</sub> with simulation cells containing up to 4 formula units were performed at 50-300 GPa by using the particle swarm optimization technique implemented in the CALYPSO code. 49,50 Structural relaxations and calculations of electronic properties were performed using the VASP code based on the density functional theory with the Perdew-Burke-Ernzerhof generalized gradient approximation. 51,52 The ion-electron interaction was described by projector-augmentedwave potentials, where  $1s^1$ ,  $3s^23p^1$ ,  $3d^{10}4s^24p^1$ ,  $3s^23p^63d^14s^2$ ,  $4s^24p^64d^15s^2$ ,  $5s^25p^65d^16s^2$ ,  $3s^23p^63d^24s^2$ ,  $4s^24p^64d^25s^2$ ,  $5p^65d^26s^2$  configurations are treated as valence electrons for H, Al, Ga, Sc, Y, La, Ti, Zr and Hf atoms, respectively.<sup>53</sup> The plane wave kinetic energy cutoff was set to 700 eV and corresponding Monkhorst-Pack (MP) k-point meshes were adopted for different structures to ensure that enthalpy converges to 1 meV/atom. Phonon calculations were performed by using the PHONOPY<sup>54</sup> or Quantum-ESPRESSO codes.<sup>55</sup> EPC calculations of  $Pm \overline{3}$  ternary hydrides were carried out with the Quantum-ESPRESSO code using ultrasoft pseudopotentials for all the atoms. A  $9\times9\times9$  q-point mesh in the first Brillouin zone (BZ) was used in the EPC calculation and a MP grid of 36×36×36 was considered to ensure k-point sampling convergence.

## III. RESULTS AND DISCUSSION

We performed structure prediction searches for twelve ternary hydrides with the AMH<sub>6</sub> composition in the pressure range of 50-300 GPa. Seven hydrides (AlTiH<sub>6</sub>, AlZrH<sub>6</sub>, AlHfH<sub>6</sub>, GaScH<sub>6</sub>, GaTiH<sub>6</sub>, GaZrH<sub>6</sub> and GaHfH<sub>6</sub>) were identified as having an A15-type structure with  $Pm\bar{3}$  symmetry, as shown in Fig. 1(a). In this structure, two metal atoms occupy the vertex and the center positions to form a bcc lattice, with H atoms occupying near their tetrahedral interstices. The A-H, M-H and H-H bond distances with  $Pm\bar{3}$  AMH<sub>6</sub> at 100 GPa are shown in Table S1. The A-H distance is shorter than the M-H distance in AlZrH<sub>6</sub> and AlHfH<sub>6</sub>, while the reverse happens in AlTiH<sub>6</sub> and GaMH<sub>6</sub>. Different metal atoms in the structure lead to two different lengths

between adjacent H atoms. The calculated H-H distances of 1.45-1.75 Å are much longer than those of 0.74 and 1.2 Å in H<sub>2</sub> and LaH<sub>10</sub> at 100 GPa, respectively, indicating that H atoms are not bonded to each other. Except for GaTiH<sub>6</sub> and GaScH<sub>6</sub>, the other five hydrides have no phase transition in the entire pressures range from 50 to 300 GPa. For GaTiH<sub>6</sub> and GaScH<sub>6</sub>, C2/m and Pmma structures were predicted to be stable at 50 GPa, respectively, and they do not present H<sub>2</sub> molecules in their structures (Fig. S1). Furthermore, AlScH<sub>6</sub> and AlYH<sub>6</sub> were predicted to have structures similar to  $Fm\bar{3}m$  Sc(Y)H<sub>3</sub>, where metal atoms form a face-centered cubic (fcc) lattice and H atoms are located at the tetrahedral and octahedral interstices of the fcc lattice. As shown in Fig. S2, Pmmn AlScH<sub>6</sub> can be seen as a 2×2×1 supercell of  $Fm\bar{3}m$  Sc(Y)H<sub>3</sub> with two metal atoms arranged alternately in two directions. P4/mmm AlScH<sub>6</sub> is formed by replacing the two Sc atoms in  $Fm\bar{3}m$  ScH<sub>3</sub> with Al atoms. I4/mmm AlYH<sub>6</sub> is similar to the P4/mmm AlScH<sub>6</sub>, but with slightly shifted H positions. The predicted structures of AlLaH<sub>6</sub>, GaYH<sub>6</sub> and GaLaH<sub>6</sub> are also shown in Figure S3.

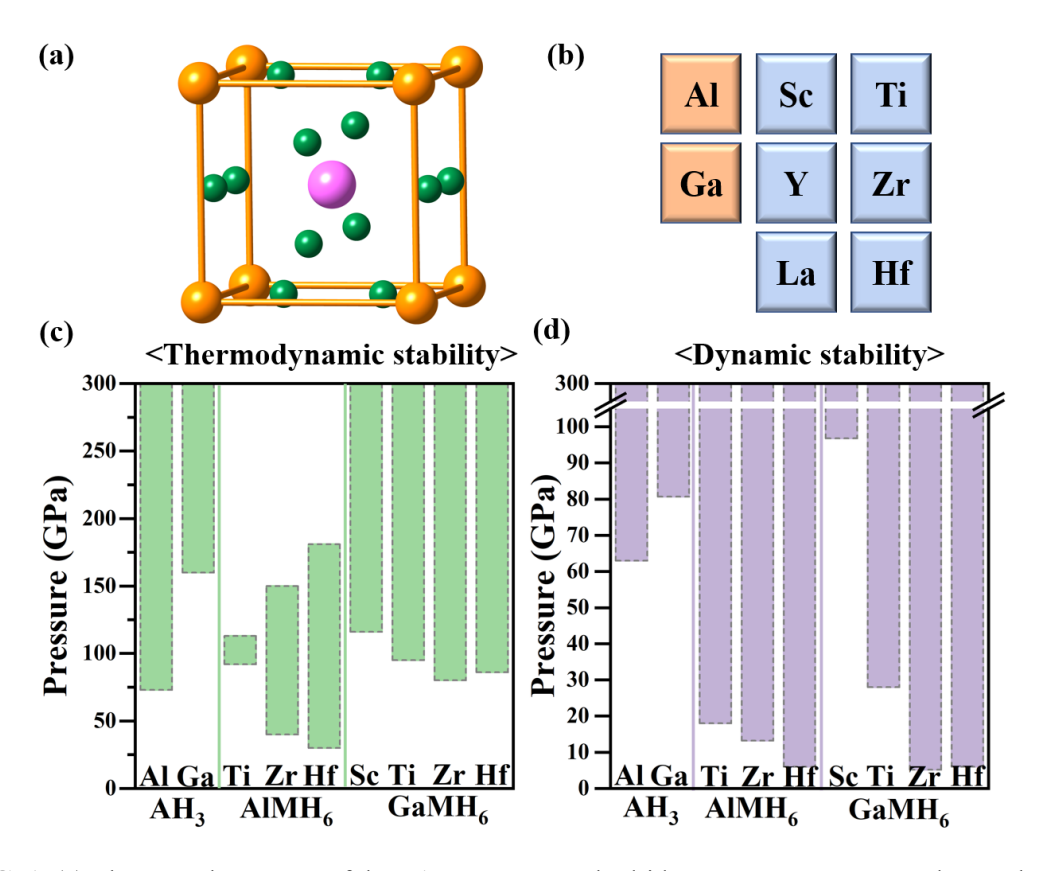


**FIG. 1.** (a) The crystal structure of the A15-type ternary hydrides. Orange, magenta and green balls represent A (Al and Ga), M (IIIB and IVB group metal) and H atom, respectively. (b) The considered

elements for the ternary hydrides. (c) Thermodynamic and (d) dynamic stability phase diagram of the  $Pm\bar{3}$  hydrides with pressure.

Bader charge analyses<sup>56</sup> were performed on A15-type ternary hydrides at 100 GPa, as shown in Table S2. The results demonstrate the transfer of electronic charges from metal to H atoms, suggesting an ionic bonding nature between them. Each H atom in AlMH<sub>6</sub> and GaMH<sub>6</sub> accepts approximately 0.60-0.64 and 0.39-0.43 e, respectively. In AIMH<sub>6</sub>, Al atoms transfer around 2.31-2.71 e to H atoms, surpassing the  $\sim$ 1.31-1.54 e transferred from the M atoms. In GaMH<sub>6</sub>, the M atom loses a greater charge (~1.34-1.61 e) compared to the Ga atom (~0.94-1.00 e), indicating a stronger ionic bonding in the M-H bond. The acquired electrons by the H<sub>2</sub> molecule occupy its antibonding orbitals, leading to an elongation of the H-H bond length and potentially even dissociation of the H<sub>2</sub> unit. In AlMH<sub>6</sub>, the significant electron transfer from Al to H atoms compensates for the relatively smaller electrons transfer from the M atom. Contrasted with GaH<sub>3</sub>, the doping M atoms enable H atoms to gain more charge in GaMH<sub>6</sub> at the same pressure, thereby allowing these ternary hydrides to exhibit structures with atomic H at lower pressures. Additionally, the electron localization functions (ELFs) were calculated for these A15 ternary hydrides at 100 GPa with an isosurface value of 0.5, as depicted in Fig. S4. The ELFs indicate that electrons are predominantly localized around the H atoms, confirming their role as electron acceptors. The ELF values below 0.5 between adjacent H atoms indicate the absence of H-H covalent bonds. The ELF values between the metal and H atoms approach zero, validating their ionic bonding character, which aligns with the aforementioned Bader charge analysis.

The thermodynamical stability of these ternary hydrides has been assessed by calculating their formation enthalpies relative to elemental solids and binary compounds. <sup>36,38-40,42-45</sup> The relative enthalpy curves for AMH<sub>6</sub> are presented in Fig. 2 and S5. The calculations consider the most stable configuration for each component and the total energy of AH<sub>3</sub> and MH<sub>3</sub> is used as the reference energy. Within certain pressure ranges, AMH<sub>6</sub> exhibits lower formation enthalpy compared to possible

decomposition pathways, indicating that AMH<sub>6</sub> is thermodynamically stable. For AlMH<sub>6</sub> (M=Ti, Zr and Hf), the predicted A15-type phases remain stable within the pressure ranges of 78-165, 69-123 and 43-157 GPa, respectively. Upon accounting for zero-point energy (ZPE), the stable pressure range for AlTiH<sub>6</sub> shrinks to 92-113 GPa and the relative formation enthalpy reduces to only -10 meV/f.u. Conversely, with ZPE corrections, the stable pressure ranges for AlZrH<sub>6</sub> and AlHfH<sub>6</sub> expand to 40-150 and 30-181 GPa, respectively. Furthermore, the stability pressure thresholds for both hydrides are lower than the 73 GPa threshold for AlH<sub>3</sub><sup>36</sup> (Fig. 1c). Regarding GaMH<sub>6</sub> (M=Sc, Ti, Zr and Hf), the predicted A15-type phases are stable above 126, 96, 85 and 95 GPa, respectively, and remain stable with increasing pressure. After considering ZPE, the minimal stable pressures change to 116, 95, 80 and 86 GPa, respectively, which are well below the stability threshold of 160 GPa for GaH<sub>3</sub> (Fig. 1c). Therefore, it is anticipated that the experimentally synthesis of A15-type GaMH<sub>6</sub> might be easier compared to GaH<sub>3</sub>. Inspired by the successful synthesis of the equal-atomic (La,Y)H<sub>4</sub> and (La,Ce)H<sub>9</sub> alloy, the high temperature and high pressure reaction of AM alloys with NH<sub>3</sub>BH<sub>3</sub> might be a promising route for the synthesis of alloy AMH<sub>6</sub>. <sup>18-19</sup> Fig. S5 demonstrates that the  $Fm\bar{3}m$  -like AlScH<sub>6</sub> is stable above 150 GPa and undergoes a transformation from the *Pmmn* phase to the P4/mmm phase at 318 GPa. The C2/m phase of AlYH<sub>6</sub> is stable above 45 GPa and transforms to the  $Fm\bar{3}m$  -like I4/mmm phase at 115 GPa. AlLaH<sub>6</sub> is predicted to exhibit the P6<sub>3</sub>/mmc and Cmcm structures below approximately 200GPa. For GaYH<sub>6</sub> and GaLaH<sub>6</sub>, the low-symmetry P2<sub>1</sub>2<sub>1</sub>2 and C2/m structures are stable near 100 GPa and below 150 GPa, respectively. Additionally, we also performed structure predictions and First-principles calculations for hydrides with higher H content in the Al-Zr-H, Ga-Sc-H, Ga-Zr-H, and Ga-Hf-H systems at 200 and 300 GPa. As shown in the Fig. S6, these H-rich hydrides have higher formation enthalpies relative to AH<sub>3</sub>+BH<sub>3</sub>+H<sub>2</sub> or AMH<sub>6</sub>+H<sub>2</sub>, indicating that they are unstable at the corresponding pressures.

To better understand the reason why the A15-type AMH<sub>6</sub> structure is stable, we conducted an analysis of the influence of the relative internal energy ( $\Delta U$ ) and the

product of pressure and volume ( $\Delta PV$ ) to the relative enthalpy ( $\Delta H$ ) under pressure. The findings for AlZrH<sub>6</sub> and AlHfH<sub>6</sub> are illustrated in Fig. S7. As pressure increases, the  $\Delta PV$  term also rises and eventually exhibits positive values. Conversely, the  $\Delta U$  term displays an opposite trend, indicating that the bonding in both ternary hydrides significantly contributes to their stabilization. For the A15-type GaMH<sub>6</sub> (Fig. S8), the  $\Delta PV$  contribution in all four hydrides is negative in comparison the benchmark, indicating that the  $\Delta PV$  term plays a dominant role in their thermodynamic stability. Meanwhile, the magnitude of  $\Delta U$  decreases with increasing pressure, leading to an overall enhancement in the stability of these ternary hydrides. Furthermore, in GaScH<sub>6</sub> the  $\Delta PV$  and  $\Delta U$  terms exhibit contrasting trends when compared to ScH<sub>3</sub>+GaH<sub>3</sub>. The negative  $\Delta PV$  contribution counteracts the negative effect of the  $\Delta U$  term, ultimately resulting in the stabilization of GaScH<sub>6</sub>. Both the  $\Delta PV$  and  $\Delta U$  contribution in GaTiH<sub>6</sub>, GaZrH<sub>6</sub> and GaHfH<sub>6</sub> have favorable effects on the thermodynamic stability relative to their respective binary hydrides.

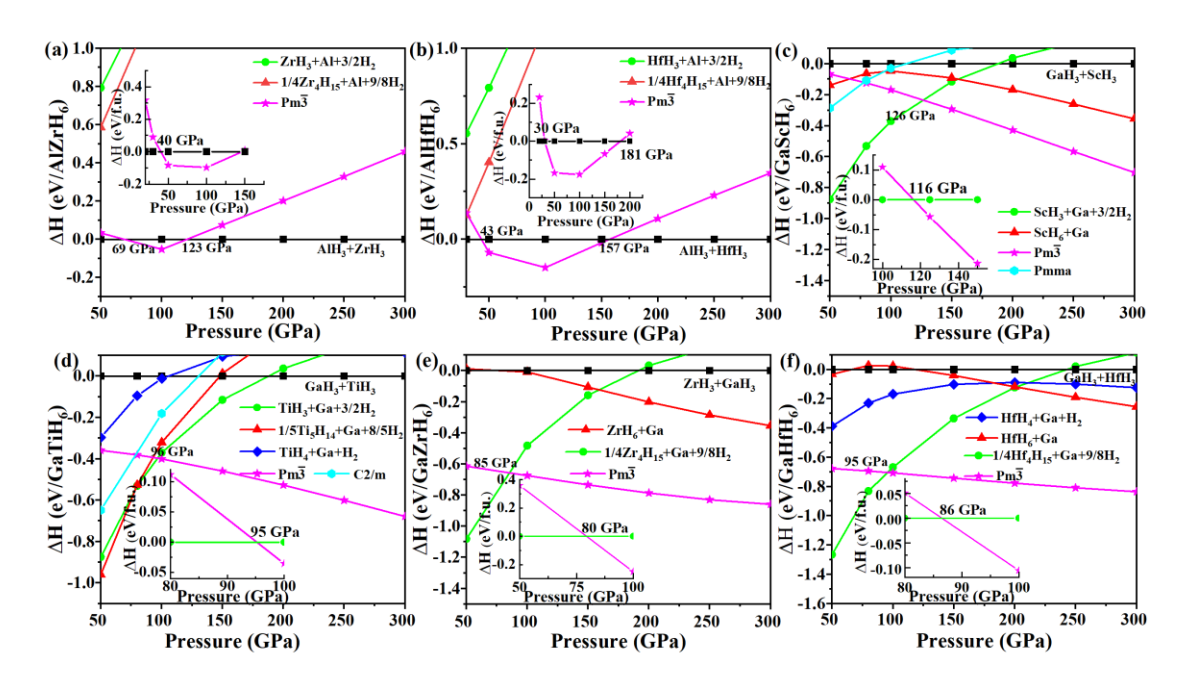


FIG. 2. The relative enthalpy curves of predicted structures for (a) AlZrH<sub>6</sub>, (b) AlHfH<sub>6</sub>, (c) GaScH<sub>6</sub>, (d) GaTiH<sub>6</sub>, (e) GaZrH<sub>6</sub> and (f) GaHfH<sub>6</sub> with respect to AH<sub>3</sub> (A=Al and Ga) and MH<sub>3</sub>(M=Sc, Ti, Zr

and Hf) under pressure. The insets show the relative enthalpies considering ZPE. The following structures for the elemental solids and binary hydrides were used for the  $\Delta H$  calculations:  $P6_3/m$ , C2/c and Cmca for H<sub>2</sub>;  $Fm\bar{3}m$  and  $P6_3/mmc$  for Al;  $Fm\bar{3}m$  for Ga;  $R\bar{3}c$ , Pnma and  $Pm\bar{3}n$  for AlH<sub>3</sub>;  $P2_1/m$  and  $Pm\bar{3}n$  for GaH<sub>3</sub>;  $Pm\bar{3}n$  and  $R\bar{3}c$  for ZrH<sub>3</sub>;  $I\bar{4}3d$  for Zr<sub>4</sub>H<sub>15</sub>,  $Cmc2_1$  and I4/mmm for ZrH<sub>6</sub>;  $Pm\bar{3}n$  for HfH<sub>3</sub>;  $I\bar{4}3d$  for Hf<sub>4</sub>H<sub>15</sub>;  $Cmc2_1$  for HfH<sub>6</sub>;  $Fm\bar{3}m$  for ScH<sub>3</sub>; Cmcm,  $P6_3/mmc$  and  $Im\bar{3}m$  for ScH<sub>6</sub>;  $Fm\bar{3}m$  for TiH<sub>3</sub>;  $I\bar{4}$  for Ti<sub>5</sub>H<sub>14</sub>; Fddd for TiH<sub>4</sub>.

We also investigated the dynamical stability of the predicted A15-type AMH<sub>6</sub> compounds by calculating the phonon spectra using the supercell approach implemented in the PHONOPY code<sup>54</sup> (Figs. S14 and S15). Within their respective thermodynamically stable pressure ranges, no imaginary frequencies were observed in the phonon spectra of these compounds, indicating their dynamically stability. Furthermore, we systematically explored the minimum pressure required for dynamical stability of these A15-type AMH<sub>6</sub>. As pressure decreases, phonon softening begins to occur, eventually leading to instability with the appearance of imaginary frequencies at certain q-wave vectors. We plotted the evolution of the frequency with pressure at the q-wave vector where the largest imaginary frequency occurs. As depicted in Figs. S9 and S10, A15-type GaScH<sub>6</sub> exhibited the highest critical pressure for dynamical stability, estimated to be around 97 GPa. GaTiH<sub>6</sub> followed with a critical pressure of approximately 28 GPa. AlTiH<sub>6</sub> and AlZrH<sub>6</sub> were found to be dynamically stable at lower pressures of about 18 and 13 GPa, respectively. Interestingly, the critical pressures of dynamical stability of AlHfH<sub>6</sub>, GaZrH<sub>6</sub> and GaHfH<sub>6</sub> were considerably lower, around 6, 5 and 6 GPa, respectively. Moreover, the threshold pressures for dynamic stability of the five ternary hydrides (GaTiH<sub>6</sub>, AlTiH<sub>6</sub>, AlHfH<sub>6</sub>, GaZrH<sub>6</sub> and GaHfH<sub>6</sub>) were much lower compared to those of AH<sub>3</sub> and MH<sub>3</sub> (Figs. S11, S13 and 1d) This suggests that these ternary hydrides could potentially be recovered at lower pressures, provided that the barriers preventing them from decomposing are sufficiently high. For Fm3m-like ternary hydrides, Pmmn AlScH<sub>6</sub>, P4/mmm AlScH<sub>6</sub> and I4/mmm AlYH<sub>6</sub> could maintain dynamically stable to 65, 139 and 43 GPa, respectively (Figs. S12 and S16).

The electronic properties of the predicted A15-type AMH<sub>6</sub> compounds were investigated at different pressures, and the results are displayed in Fig. 3, as well as Figs. S17 and S18. The calculated density of states (DOS) reveals the presence of electronic states at the Fermi energy level  $(E_f)$ , indicating that these hydrides exhibit metallic behavior within the studied pressure range. The contributions of the metal and hydrogen atoms to the total DOS are also depicted in the figures. Fig. 3d highlights a distinct difference between the DOS of GaScH<sub>6</sub> and the other six hydrides composed of Al/Ga and group IVB metals. In GaScH<sub>6</sub>, the hydrogen atoms significantly contribute to the DOS at the  $E_f$ , suggesting the potential for excellent superconducting properties. In the remaining six hydrides, the group IVB metals have one additional valence electron compared to Sc atoms, causing a shift of the E<sub>f</sub> to higher energies relative to GaScH<sub>6</sub>. These six hydrides exhibit higher or comparable total DOS at the  $E_f$  compared to GaScH<sub>6</sub>. However, the DOS contributions from Al and Ga atoms are relatively lower due to significant charge transfer to the H atoms. In the case of the group IVB metals, the DOS at  $E_f$  is mainly contributed by d orbitals. Furthermore, the electronic band structures of AlHfH<sub>6</sub>, GaScH<sub>6</sub> and GaZrH<sub>6</sub> were examined as examples at pressures of 10, 100 and 10 GPa, respectively. The band projections onto different elements are also displayed in the band structures. In these three hydrides, a band associated with Al/Ga atoms is observed to cross the  $E_f$  steeply along the M-R- $\Gamma$  direction. Additionally, in AlHfH<sub>6</sub> and GaZrH<sub>6</sub> there is an electron pocket at the M point and a flat band along the  $\Gamma$ -M direction, dominated by Hf and Zr atoms, located near the  $E_f$ . In the case of GaScH<sub>6</sub>, electron and hole pockets are observed along the X-M direction, along with a flat band along the  $\Gamma$ -M direction, which are attributed to H atoms. These localized electronic states contribute to a high DOS at the Fermi energy and play a role in electron-phonon interactions. Moreover, a comparison was made between the DOS of A15-type AlH<sub>3</sub>, AlTiH<sub>6</sub>, AlZrH<sub>6</sub> and AlHfH<sub>6</sub> at 100 GPa. As shown in Fig. S17, the DOS at E<sub>f</sub> for AlTiH<sub>6</sub>, AlZrH<sub>6</sub> and AlHfH<sub>6</sub> are 0.030, 0.018 and 0.018 states/eV/Å<sup>3</sup> respectively, which are significantly higher than that of AlH<sub>3</sub> (0.008 states/eV/Å<sup>3</sup>). The doping of AlH<sub>3</sub> with Ti, Zr and Hf atoms elevated the  $E_f$ , resulting in an increased DOS at the  $E_f$ .

Ternary hydrides exhibit a more pronounced metallic character compared to AlH<sub>3</sub>, potentially enhancing their superconducting properties.

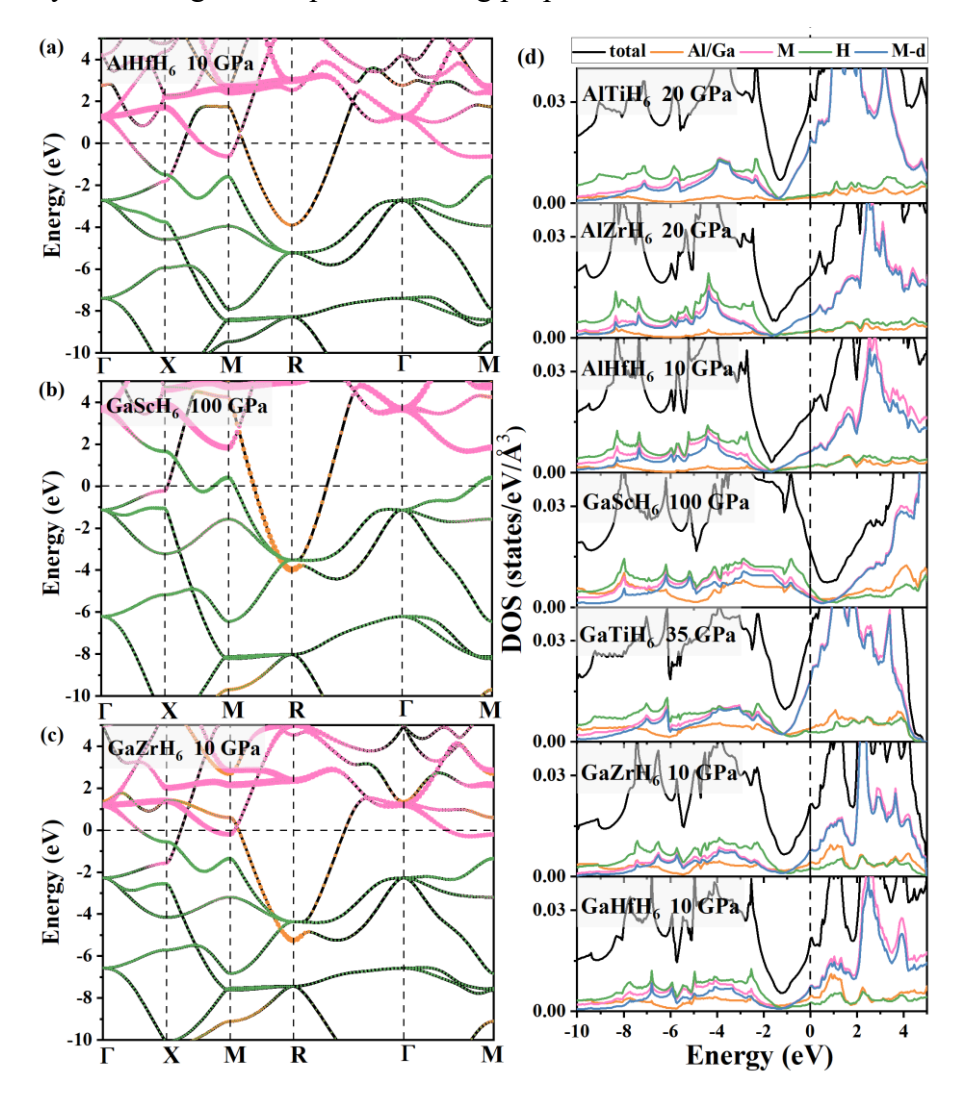


FIG. 3. The calculated band structures and electronic density of states of  $Pm\overline{3}$  ternary hydrides at different pressures.

After determining the stability and metallicity of A15-type ternary hydrides, we conducted EPC calculations to investigate their superconductivity. The calculated phonon dispersion curves, projected phonon density of states (PDOS), Eliashberg phonon spectral function  $\alpha^2 F(\omega)/\omega$ , and its integral  $\lambda(\omega)$  for  $Pm\bar{3}$  AlHfH<sub>6</sub>, GaScH<sub>6</sub> and GaZrH<sub>6</sub> at pressures of 10, 100 and 10 GPa are displayed in Fig. 4. From the PDOS, it is evident that the high-frequency and low-frequency phonon modes are associated with the vibration of H and metal atoms, respectively. The right panels of Fig. 4 illustrate that the peaks of  $\alpha^2 F(\omega)/\omega$  for AlHfH<sub>6</sub>, GaScH<sub>6</sub> and GaZrH<sub>6</sub> are predominantly

distributed below 15, 20 and 15 THz, respectively, with the corresponding  $\lambda(\omega)$  increasing rapidly. The EPC strength on the different phonon modes is also depicted on the phonon dispersions. As a result, the significant contribution to the EPC comes from the soft modes associated with H-atom vibrations and the modes dominated by metal atoms. This leads to a total EPC parameter  $\lambda$  of 2.18, 1.56 and 1.80 for AlHfH<sub>6</sub>, GaScH<sub>6</sub> and GaZrH<sub>6</sub> at pressures of 10, 100 and 10 GPa, respectively.

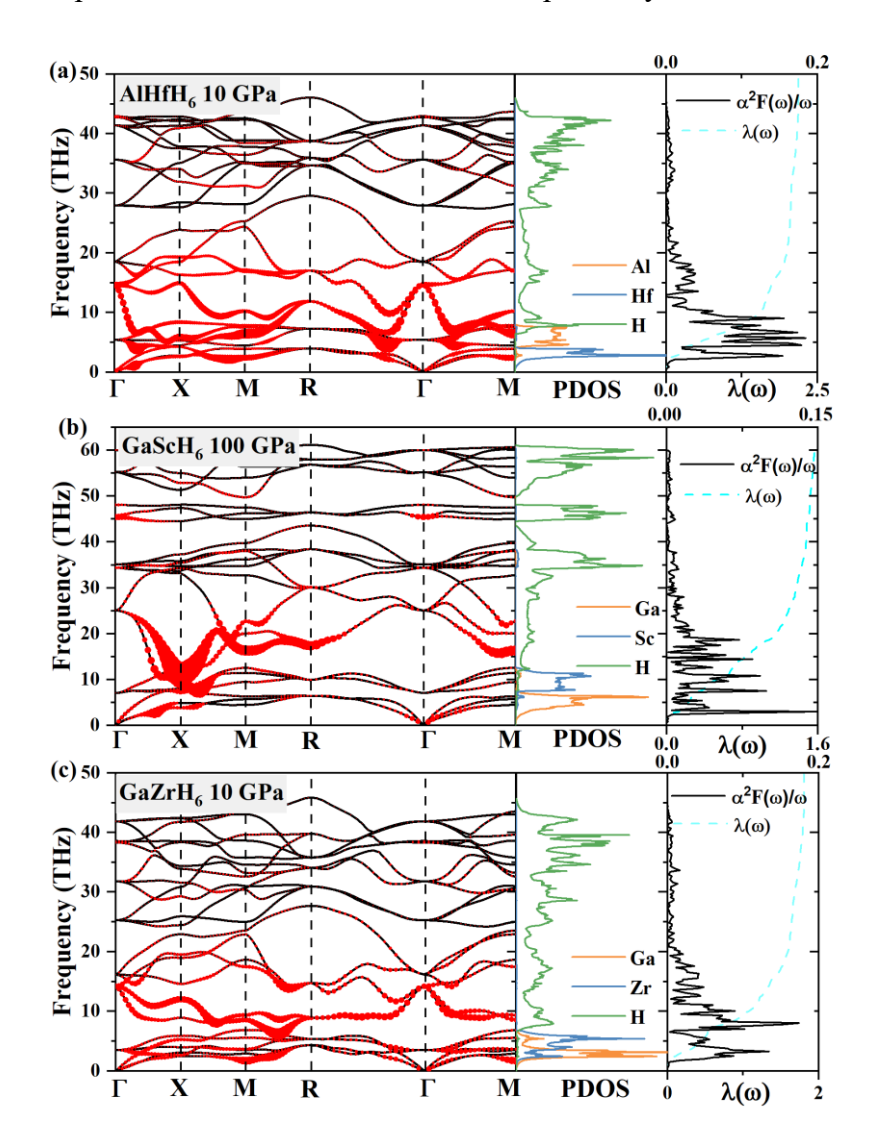


FIG. 4. Calculated phonon dispersion curves (the area of the red circles is proportional to the EPC strength), projected phonon density of states (PDOS), the Eliashberg phonon spectral function  $\alpha^2 F(\omega)/\omega$  and its integral  $\lambda(\omega)$  for (a)  $Pm\bar{3}$  AlHfH<sub>6</sub> at 10 GPa, (b)  $Pm\bar{3}$  GaScH<sub>6</sub> at 100 GPa and (c)  $Pm\bar{3}$  GaZrH<sub>6</sub> at 10 GPa.

The superconducting critical temperature for the predicted A15-type ternary

hydrides were calculated using the Allen-Dynes modified McMillan equation with a Coulomb pseudopotential parameter ( $\mu^*$ ) ranging from 0.1 to 0.13.<sup>57</sup> The calculated  $T_c$ values, along with the EPC parameter  $\lambda$  and the phonon frequency logarithmic average  $\omega_{\log}$  are presented in Fig. 5 and Table 1. For AlTiH<sub>6</sub>, the calculated EPC parameter  $\lambda$  is 1.15 and the phonon frequency logarithmic average  $\omega_{\log}$  is 423 K. This results in a  $T_c$  of 32-36 K at 20 GPa. AlZrH<sub>6</sub> and AlHfH<sub>6</sub> present stronger EPC interactions, with  $\lambda$  of 1.72 and 2.18, and the  $T_c$  values are estimated to be 59-64 and 57-60 K at 20 and 10 GPa, respectively. Considering that the  $\lambda$  values are higher than 1.5, the calculated  $T_c$ values are further rectified with the strong coupling  $(f_1)$  and shape correction  $(f_2)$  and improved to be 68-75 and 70-76 K, respectively. The T<sub>c</sub> values obtained for AlMH<sub>6</sub> are indeed higher than those of AlH<sub>3</sub> and the corresponding MH<sub>3</sub> compounds.<sup>37,39,40,45</sup> Similarly, GaScH<sub>6</sub> exhibits the highest  $T_c$  among the studied hydrides, reaching a range of 79-88 K at a higher pressure of 100 GPa, However, its  $T_c$  is slightly lower than that of GaH<sub>3</sub>, which has a T<sub>c</sub> of 102 K of at 120 GPa. In case of GaTiH<sub>6</sub>, it shows a lower T<sub>c</sub> range of 34-39 K at 35 GPa compared to the T<sub>c</sub> of 63-70 K for GaZrH<sub>6</sub> and 45-49 K for GaHfH6 at 10 GPa.

The evolution of  $T_c$  with pressure was also investigated for  $Pm\overline{3}$  AMH<sub>6</sub>. For AlZrH<sub>6</sub>, the calculated EPC parameter  $\lambda$  decreased from 1.72 at 20 GPa to 1.18 at 30 GPa, while the  $\omega_{log}$  increased from 494 to 667 K, resulting in a slight decrease in the  $T_c$  with  $\mu^*$  of 0.1 from 64 to 59 K (Allen-Dynes modified McMillan equation). Similarly, as the pressure increased from 10 to 20 GPa, the  $\lambda$  for AlHfH<sub>6</sub> decreased from 2.18 to 1.28 and the  $\omega_{log}$  increased from 397 to 596 K. As a result, the calculated  $T_c$  with  $\mu^*$  of 0.1 decreased slightly from 60 to 58 K. The increase in pressure leads to a stiffening of the phonon modes, which results in a decrease in EPC parameter and an increase in  $\omega_{log}$ . This compensating effect prevents a significant reduction in  $T_c$ . In addition, the  $T_c$  values of GaMH<sub>6</sub> compounds decrease with increasing pressure, due to the competition between the descending EPC parameter ( $\lambda$ ) and the increasing phonon frequency logarithmic average ( $\omega_{log}$ ). For  $Fm\overline{3}m$ -like ternary hydrides, Pmmn AlScH<sub>6</sub>, P4/mmm AlScH<sub>6</sub> and I4/mmm AlYH<sub>6</sub> found to be metallic (Fig. S19) and subsequent EPC

calculations suggest that they exhibit superconductivity. The  $T_c$  values for these hydrides are estimated to be 42, 32 and 52 K at pressures of 80, 200 and 60 GPa, respectively (Table S3).

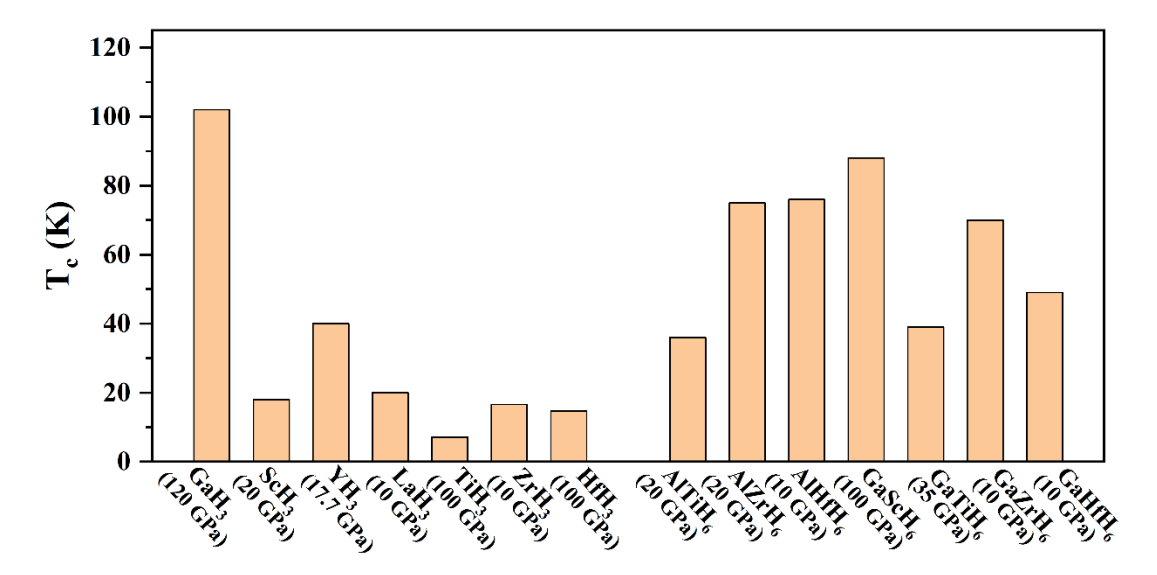


FIG. 5. The estimated  $T_c$  for the predicted A15 AMH<sub>6</sub> using the Allen-Dynes modified McMillan equation and for already known A(M)H<sub>3</sub> compounds extracted from literature.<sup>38-40,43-45</sup>

Table 1. The calculated values for electron-phonon coupling parameter  $\lambda$ , phonon frequency logarithmic average  $\omega_{\log}$ , critical temperature  $T_c$  ( $\mu^*=0.1\text{-}0.13$ ) using the Allen-Dynes modified McMillan equation without and with strong-coupling and shape corrections for  $Pm\overline{3}$  ternary hydrides.

Phase	Pressure	λ	ωlog	$T_{c}\left(\mathbf{K}\right)$	$T_c$ (K) with $f_l$ and $f_2$
	(GPa)			μ*=0.1-0.13	$\mu$ *=0.1-0.13
AlTiH <sub>6</sub>	20	1.15	423	32-36	
AlZrH <sub>6</sub>	20	1.72	494	59-64	68-75
	30	1.18	667	52-59	
AlHfH <sub>6</sub>	10	2.18	397	57-60	70-76
	20	1.28	596	52-58	
GaScH <sub>6</sub>	100	1.56	641	69-76	79-88

	120	1.09	890	71-62	
$GaTiH_6$	35	1.17	448	34-39	
	100	0.68	887	29-22	
GaZrH <sub>6</sub>	10	1.80	438	54-58	63-70
	80	0.81	898	43-35	
GaHfH <sub>6</sub>	10	1.42	454	45-49	
	86	0.74	802	32-25	

#### IV. CONCLUSIONS

In summary, we have carried out crystal structural prediction and first-principles calculations on alloy hydrides with the AMH<sub>6</sub> composition under pressure. Seven ternary hydrides, AlMH<sub>6</sub> (M=Ti, Zr and Hf) and GaMH<sub>6</sub> (M=Sc, Ti, Zr and Hf) were predicted to adopt the A15-type structure, and the calculated enthalpy curves indicated that the A15-type AlMH<sub>6</sub> are stable within specific pressure ranges of 92-113, 40-150 and 30-181, respectively. The onset stable pressures for AlZrH<sub>6</sub> and AlHfH<sub>6</sub> are lower than the stability threshold of 73 GPa for AlH<sub>3</sub>. Phonon calculations demonstrated that A15-type AlTiH<sub>6</sub>, AlZrH<sub>6</sub>, AlHfH<sub>6</sub> can be dynamically stable at relatively low pressures, such as, 18, 13 and 6 GPa, respectively. Additionally, the addition of Ti, Zr and Hf into AlH<sub>3</sub> influenced the position of the Fermi level, resulting in improved metallicity compared to AlH<sub>3</sub>. Consequently, the ternary hydrides exhibited higher T<sub>c</sub>s of 36, 75 and 76 K at 20, 20 and 10 GPa, respectively. The A15-type GaMH<sub>6</sub> hydrides (GaScH<sub>6</sub>, GaTiH<sub>6</sub>, GaZrH<sub>6</sub>, and GaHfH<sub>6</sub>) were found to have minimum thresholds of thermodynamically stable pressure at 116, 95, 80 and 86 GPa respectively, which are significantly lower than the stability threshold of 160 GPa for GaH<sub>3</sub>. Additionally, dynamical stability calculations indicated their potential retention down to lower pressures of 97, 28, 5 and 6 GPa, respectively. EPC calculations revealed that A15-type GaMH<sub>6</sub> hydrides are superconducting, with T<sub>c</sub>s of 88, 39, 70 and 49 K at 100, 35, 10 and 10 GPa, respectively. AlScH<sub>6</sub> and AlYH<sub>6</sub> were predicted to be stable in Fm3m  $Sc(Y)H_3$ -like structures under pressure. The estimated  $T_c$  values for Pmmn, P4/mmm

AlScH<sub>6</sub> and I4/mmm AlYH<sub>6</sub> were 42, 32 and 52 K at 80, 200 and 60 GPa, respectively. These findings suggest that alloying holds promise as a route to lower the stabilization pressure of hydrides, enabling the exploration of high- $T_c$  hydride superconductors that can be stable at lower or ambient pressures.

#### **SUPPLEMENTARY MATERIAL**

See supplementary material for the predicted structures of GaTiH<sub>6</sub>, GaScH<sub>6</sub>, AlScH<sub>6</sub>, AlYH<sub>6</sub>, AlLaH<sub>6</sub>, GaYH<sub>6</sub> and GaLaH<sub>6</sub>; ELFs; the relative enthalpy curves of AlTiH<sub>6</sub>, AlScH<sub>6</sub>, AlYH<sub>6</sub>, AlLaH<sub>6</sub>, GaYH<sub>6</sub> and GaLaH<sub>6</sub>; The formation enthalpies of hydrides with higher H content in the Al-Zr-H, Ga-Sc-H, Ga-Zr-H and Ga-Hf-H system with respect to decomposition into AH<sub>3</sub>+BH<sub>3</sub>+H<sub>2</sub> or AMH<sub>6</sub>+H<sub>2</sub> at 200 and 300 GPa; the relative internal energies ΔU and ΔPV components of the enthalpy for the A15 ternary hydrides; the evolution of the frequency with pressure for the studied hydrides; phonon spectra, electronic density of states, structural information; Bader charge analyses; superconductivity of the *Pmmn*, *P*4/*mmm* AlScH<sub>6</sub> and *I*4/*mmm* AlYH<sub>6</sub>.

#### **ACKNOWLEDGMENTS**

This work was supported by Natural Science Foundation of China (Grant Nos. 52022089, 52090020, 52288102 and 11964026), the National Key R&D Program of China (2022YFA1402300, 2018YFA0703400), the Natural Science Foundation of Hebei Province (E2022203109), P.F. Li thanks Science and Technology Leading Talents and Innovation Team Building Projects of Inner Mongolia Autonomous Region (GXKY22060). A.B. acknowledges financial support from the Spanish Ministry of Science and Innovation (Grant No. FIS2019-105488GB-I00) and the Department of Education, Universities and Research of the Basque Government and the University of the Basque Country (IT1707-22). E. Z. acknowledges the National Science Foundation (DMR-2136038) for financial support.

#### AUTHOR DECLARATIONS

# **Conflict of Interest**

The authors have no conflicts to disclose.

# **DATA AVAILABILITY**

The data supporting the findings of this study are publicly available from the corresponding author upon request.

#### REFERENCES

- <sup>1</sup>J. A. Flores-Livas, L. Boeri, A. Sanna, G. Profeta, R. Arita, and M. Eremets, "A perspective on conventional high-temperature superconductors at high pressure: Methods and materials," Phys. Rep. **856**, 1 (2020).
- <sup>2</sup>D. V. Semenok, I. A. Kruglov, I. A. Savkin, A. G. Kvashnin, and A. R. Oganov, "On Distribution of Superconductivity in Metal Hydrides," Curr. Opin. Solid State Mater. Sci. **24**, 100808 (2020).
- <sup>3</sup>H. Wang, X. Li, G. Gao, Y. Li, and Y. Ma, "Hydrogen-rich superconductors at high pressures," Wiley Interdiscip. Rev: Comput. Mol. Sci. **8**, e1330 (2018).
- <sup>4</sup>K. P. Hilleke and E. Zurek, "Tuning chemical precompression: Theoretical design and crystal chemistry of novel hydrides in the quest for warm and light superconductivity at ambient pressures," J. Appl. Phys. **131**, 070901 (2022).
- <sup>5</sup>G. Gao, L. Wang, M. Li, J. Zhang, R. T. Howie, E. Gregoryanz, V. V. Struzhkin, L. Wang, and J. S. Tse, "Superconducting binary hydrides: Theoretical predictions and experimental progresses," Mater. Today Phys. **21**, 100546 (2021).
- <sup>6</sup>M. I. Eremets, V. S. Minkov, A. P. Drozdov, P. P. Kong, V. Ksenofontov, S. I. Shylin, S. L. Bud'ko, R. Prozorov, F. F. Balakirev and Dan Sun *et al.*, "High-Temperature Superconductivity in Hydrides: Experimental Evidence and Details," J Supercond. Nov. Magn. **35**, 965 (2022).
- <sup>7</sup>A. P. Drozdov, M. I. Eremets, I. A. Troyan, V. Ksenofontov, and S. I. Shylin, "Conventional superconductivity at 203 kelvin at high pressures in the sulfur hydride system," Nature **525**, 73 (2015).
- <sup>8</sup>M. Einaga, M. Sakata, T. Ishikawa, K. Shimizu, M. I. Eremets, A. P. Drozdov, I. A. Troyan, N. Hirao, and Y. Ohishi, "Crystal structure of the superconducting phase of sulfur hydride," Nat. Phys. 12, 835 (2016).
- <sup>9</sup>A. P. Drozdov, P. P. Kong, V. S. Minkov, S. P. Besedin, M. A. Kuzovnikov, S. Mozaffari, L. Balicas, F. F. Balakirev, D. e. Graf and V. B. Prakapenka *et al.*, "Superconductivity at 250 K in lanthanum hydride under high pressures," Nature **569**, 528 (2019).
- <sup>10</sup>M. Somayazulu, M. Ahart, A. K. Mishra, Z. M. Geballe, M. Baldini, Y. Meng, V. V. Struzhkin, and R. J. Hemley, "Evidence for Superconductivity above 260 K in Lanthanum Superhydride at Megabar Pressures," Phys. Rev. Lett. **122**, 027001 (2019).
- <sup>11</sup>D. V. Semenok, A. G. Kvashnin, A. G. Ivanova, V. Svitlyk, V. Yu. Fominski, A.V. Sadakov, O.A. Sobolevskiy, V. M. Pudalov, I.A. Troyan and A. R. Oganov, "Superconductivity at 161 K in thorium hydride ThH<sub>10</sub>: Synthesis and properties," Mater. Today **33**, 36 (2020).
- <sup>12</sup>I. A. Troyan, D. V. Semenok, A. G. Kvashnin, A. V. Sadakov, O. A. Sobolevskiy, V. M. Pudalov, A. G. Ivanova, V. B. Prakapenka, E. Greenberg and A. G. Gavriliuk *et al.*, "Anomalous High-Temperature Superconductivity in YH<sub>6</sub>," Adv. Mater. **33**, 2006832 (2021).
- <sup>13</sup>P. Kong, V. S. Minkov, M.A. Kuzovnikov, A. P. Drozdov, S. P. Besedin, S. Mozaffari, L. Balicas, F. F. Balakirev, V. B. Prakapenka and S. Chariton et al., "Superconductivity up to 243 K in the yttriumhydrogen system under high pressure," Nature Commun. **12**, 5075 (2021).
- <sup>14</sup>E. Snider, N. Dasenbrock-Gammon, R. McBride, X. Wang, N. Meyers, K. V. Lawler, E. Zurek, A. Salamat, and R. P. Dias, "Synthesis of Yttrium Superhydride Superconductor with a Transition Temperature up to 262 K by Catalytic Hydrogenation at High Pressures," Phys. Rev. Lett. **126**, 117003 (2021).
- <sup>15</sup>L. Ma, K. Wang, Y. Xie, X. Yang, Y. Wang, M. Zhou, H. Liu, X. Yu, Y. Zhao and H. Wang *et al.*, "High-Temperature Superconducting Phase in Clathrate Calcium Hydride CaH<sub>6</sub> up to 215 K at a

- Pressure of 172 GPa," Phys. Rev. Lett. 128, 167001 (2022).
- <sup>16</sup>Z. Li, X. He, C. Zhang, X. Wang, S. Zhang, Y. Jia, S. Feng, K. Lu, J. Zhao, J. Zhang *et al.*, "Superconductivity above 200 K discovered in superhydrides of calcium," Nature Commun. **13**, 2863 (2022).
- <sup>17</sup>D. V. Semenok, I. A. Troyan, A. G. Ivanova, A. G. Kvashnin, I. A. Kruglov, M. Hanfland,
- A. V. Sadakov, O. A. Sobolevskiy, K. S. Pervakov and I. S. Lyubutin *et al.*, "Superconductivity at 253 K in lanthanum yttrium ternary hydrides," Mater. Today **48**, 18 (2021).
- <sup>18</sup>J. Bi, Y. Nakamoto, P. Zhang, Y. Wang, L. Ma, Y. Wang, B. Zou, K. Shimizu, H. Liu and M. Zhou *et al.*, "Stabilization of superconductive La–Y alloy superhydride with Tc above 90 K at megabar pressure," Mater. Today Phys. **28**, 100840 (2022).
- <sup>19</sup>J. Bi, Y. Nakamoto, P. Zhang, K. Shimizu, B. Zou, H. Liu, M. Zhou, G. Liu, H. Wang and Y. Ma, "Giant enhancement of superconducting critical temperature in substitutional alloy (La,Ce)H<sub>9</sub>," Nature Commun. **13**, 5952 (2022).
- <sup>20</sup>S. Chen, Y. Qian, X. Huang, W. Chen, J. Guo, K. Zhang, J. Zhang, H. Yuan, T. Cui, "High-temperature superconductivity up to 223 K in the Al stabilized metastable hexagonal lanthanum superhydride," Natl. Sci. Rev. nwad107, (2023).
- <sup>21</sup>X. Li, X. Huang, D. Duan, C. J. Pickard, D. Zhou, H. Xie, Q. Zhuang, Y. Huang, Q. Zhou and B. Liu *et al.*, "Polyhydride CeH<sub>9</sub> with an atomic-like hydrogen clathrate structure," Nature Commun. **10**, 3461 (2019).
- <sup>22</sup>N. P. Salke, M. Mahdi Davari Esfahani, Y. Zhang, I. A. Kruglov, J. Zhou, Y. Wang, E. Greenberg, V. B. Prakapenka, J. Liu and A. R. Oganov *et al.*, "Synthesis of clathrate cerium superhydride CeH<sub>9</sub> at 80-100 GPa with atomic hydrogen sublattice" Nature Commun. **10**, 4453 (2019).
- <sup>23</sup>H. Wang, J. S. Tse, K. Tanaka, T. Iitaka, and Y. Ma, "Superconductive sodalite-like clathrate calcium hydride at high pressures," Proc. Natl. Acad. Sci. **109**, 6463 (2012).
- <sup>24</sup>Y. Li, J. Hao, H. Liu, J. S. Tse, Y. Wang, and Y. Ma, "Pressure-stabilized superconductive yttrium hydrides," Sci. Rep. **5**, 9948 (2015).
- <sup>25</sup>H. Liu, I. I. Naumov, R. Hoffmann, N. W. Ashcroft, and R. J. Hemley, "Potential high-T<sub>c</sub> superconducting lanthanum and yttrium hydrides at high pressure," Proc. Natl. Acad. Sci. **114**, 6990 (2017).
- <sup>26</sup>F. Peng, Y. Sun, C. J. Pickard, R. J. Needs, Q. Wu, and Y. Ma, "Hydrogen Clathrate Structures in Rare Earth Hydrides at High Pressures: Possible Route to Room-Temperature Superconductivity," Phys. Rev. Lett. **119**, 107001 (2017).
- <sup>27</sup>X. Liang, A. Bergara, L. Wang, B. Wen, Z. Zhao, X.-F. Zhou, J. He, G. Gao, and Y. Tian, "Potential high-T<sub>c</sub> superconductivity in CaYH<sub>12</sub> under pressure," Phys. Rev. B **99**, 100505 (2019).
- <sup>28</sup>T. Ishikawa, T. Miyake, and K. Shimizu, "Materials informatics based on evolutionary algorithms: Application to search for superconducting hydrogen compounds" Phys. Rev B **100**, 174506 (2019).
- <sup>29</sup>X. Liang, A. Bergara, X. Wei, X. Song, L. Wang, R. Sun, H. Liu, R. J. Hemley, L. Wang and G.Gao *et al.*, "Prediction of high-T<sub>c</sub> superconductivity in ternary lanthanum borohydrides," Phys. Rev. B **104**, 134501 (2021).
- <sup>30</sup>Z. Zhang, T. Cui, M. J. Hutcheon, A. M. Shipley, H Song, M. Du, V. Z. Kresin, D. Duan, C. J. Pickard and Y. Yao, "Design Principles for High-Temperature Superconductors with a Hydrogen-Based Alloy Backbone at Moderate Pressure," Phys. Rev. Lett. **128**, 047001 (2022).
- <sup>31</sup>S. Di Cataldo, C. Heil, W. von der Linden, and L. Boeri, "LaBH<sub>8</sub>: Towards high-Tc low-pressure superconductivity in ternary superhydrides," Phys. Rev. B **104**, L020511 (2021).

- <sup>32</sup>R. Lucrezi, S. Di Cataldo, W. von der Linden, L. Boeri, and C. Heil, "In-silico synthesis of lowest-pressure high-Tc ternary superhydrides," npj Comput. Mater. **8**, 119 (2022).
- <sup>33</sup>Y. Sun, S. Sun, X. Zhong, and H. Liu, "Prediction for high superconducting ternary hydrides below megabar pressure," J. Phys.: Condens. Matter **34**, 505404 (2022).
- $^{34}$ M. Gao, X.-W. Yan, Z.-Y. Lu, and T. Xiang, "Phonon-mediated high-temperature superconductivity in the ternary borohydride KB<sub>2</sub>H<sub>8</sub> under pressure near 12 GPa," Phys. Rev. B **104**, L100504 (2021).
- <sup>35</sup>M.-J. Jiang, Y.-L. Hai, H.-L. Tian, H.-B. Ding, Y.-J. Feng, C.-L. Yang, X.-J. Chen, and G.-H. Zhong, "High-temperature superconductivity below 100 GPa in ternary C-based hydride MC<sub>2</sub>H<sub>8</sub> with molecular crystal characteristics (M= Na, K, Mg, Al, and Ga)," Phys. Rev. B **105**, 104511 (2022).
- <sup>36</sup>C. J. Pickard and R. J. Needs, "Metallization of aluminum hydride at high pressures: A first-principles study," Phys. Rev. B **76**, 144114 (2007).
- <sup>37</sup>I. Goncharenko, M. I. Eremets, M. Hanfland, J. S. Tse, M. Amboage, Y. Yao, and I. A. Trojan, "Pressure-Induced Hydrogen-Dominant Metallic State in Aluminum Hydride," Phys. Rev. Lett. **100**, 045504 (2008).
- <sup>38</sup>G. Gao, H. Wang, A. Bergara, Y. Li, G. Liu, and Y. Ma, "Metallic and superconducting gallane under high pressure," Phys. Rev. B **84**, 064118 (2011).
- <sup>39</sup>H. Xie, W. Zhang, D. Duan, X. Huang, Y. Huang, H. Song, X. Feng, Y. Yao, C. J. Pickard and T. Cui, "Superconducting Zirconium Polyhydrides at Moderate Pressures," J Phys. Chem. Lett. **11**, 646 (2020).
- <sup>40</sup>H. Xie, Y. Yao, X. Feng, D. Duan, H. Song, Z.Zhang, S. Jiang, S. A. T. Redfern, V. Z. Kresin and C. J. Pickard *et al.*, "Hydrogen Pentagraphenelike Structure Stabilized by Hafnium: A High-Temperature Conventional Superconductor," Phys. Rev. Lett. **125**, 217001 (2020).
- <sup>41</sup>B. Rousseau and A. Bergara, "Giant anharmonicity suppresses superconductivity in AlH<sub>3</sub> under pressure," Phys. Rev. B **82**, 104504 (2010).
- <sup>42</sup>X. Ye, R. Hoffmann, and N. W. Ashcroft, "Theoretical Study of Phase Separation of Scandium Hydrides under High Pressure," J Phys. Chem. C **119**, 5614 (2015).
- <sup>43</sup>D. Y. Kim, R. H. Scheicher, H.-k. Mao, T. W. Kang, and R. Ahuja, "General trend for pressurized superconducting hydrogen-dense materials," Proc. Natl. Acad. Sci. **107**, 2793 (2010).
- <sup>44</sup>D. Y. Kim, R. H. Scheicher, and R. Ahuja, "Predicted High-Temperature Superconducting State in the Hydrogen-Dense Transition-Metal Hydride YH<sub>3</sub> at 40 K and 17.7 GPa," Phys. Rev. Lett. **103**, 077002 (2009).
- <sup>45</sup>J. Zhang, J. M. McMahon, A. R. Oganov, X. Li, X. Dong, H. Dong, and S. Wang, "High-temperature superconductivity in the Ti-H system at high pressures," Phys. Rev. B **101**, 134108 (2020).
- <sup>46</sup>G. R. Stewart, "Superconductivity in the A15 structure," Physica C: Superconductivity and its Applications **514**, 28 (2015).
- <sup>47</sup>X. Wei , X.Hao, A. Bergara, E. Zurek, X.Liang, L. Wang, X. Song, P. Li, L. Wang, G. Gao, and Y. Tian, "Designing ternary superconducting hydrides with A15-type structure at moderate pressures," Mater. Today Phys., **34**, 101086 (2023).
- <sup>48</sup>W. Zhao, H. Song, M. Du, Q. Jiang, T. Ma, M. Xu, D. Duan, and T. Cui, "Pressure-induced high-temperaturesuperconductivity in ternary Y-Zr-H compound," Phys. Chem. Chem. Phys. **25**, 5237 (2023).

- <sup>49</sup>Y. Wang, J. Lv, L. Zhu, and Y. Ma, "Crystal structure prediction via particle-swarm optimization," Phys. Rev. B **82**, 094116 (2010).
- <sup>50</sup>Y. Wang, J. Lv, L. Zhu, and Y. Ma, "CALYPSO: A method for crystal structure prediction," Comput. Phys. Commun. **183**, 2063 (2012).
- <sup>51</sup>G. Kresse and J. Furthmüller, "Efficient iterative schemes for ab initio total-energy calculations using a plane-wave basis set," Phys. Rev. B **54**, 11169 (1996).
- <sup>52</sup>J. P. Perdew, K. Burke, and M. Ernzerhof, "Generalized Gradient Approximation Made Simple," Phys. Rev. Lett. 77, 3865 (1996).
- <sup>53</sup>P. E. Blöchl, "Projector augmented-wave method," Phys. Rev. B **50**, 17953 (1994).
- <sup>54</sup>A. Togo, F. Oba, and I. Tanaka, "First-principles calculations of the ferroelastic transition between rutile-type and CaCl<sub>2</sub>-type SiO<sub>2</sub> at high pressures," Phys. Rev. B **78**, 134106 (2008).
- <sup>55</sup>P. Giannozzi, S. Baroni, N. Bonini, M. Calandra, R. Car, C. Cavazzoni, D. Ceresoli, G. L. Chiarotti, M. Cococcioni, I. Dabo, A. Dal Corso, S. de Gironcoli, S. Fabris, G. Fratesi, R. Gebauer, U. Gerstmann, C. Gougoussis, A. Kokalj, M. Lazzeri, L. Martin-Samos, N. Marzari, F. Mauri, R. Mazzarello, S. Paolini, A. Pasquarello, L. Paulatto, C. Sbraccia, S. Scandolo, G. Sclauzero, A. P. Seitsonen, A. Smogunov, P. Umari, and R. M. Wentzcovitch, "QUANTUM ESPRESSO: A modular and open-source software project for quantum simulations of materials," J. Phys.: Condens. Matter 21, 395502 (2009).
- <sup>56</sup>R. Bader, Atoms in Molecules: A Quantum Theory (Oxford University Press, Oxford, 1994)
- <sup>57</sup>P. B. Allen and R. C. Dynes, "Transition temperature of strong-coupled superconductors reanalyzed," Phys. Rev. B **12**, 905 (1975).